Tanzania Journal of Science 48(3): 691-702, 2022
ISSN 0856-1761, e-ISSN 2507-7961

Mineralogy and Geochemistry of the Asanje Iron Ore Deposit within the Mayamaya-Hombolo Belt, Dodoma Region, Central Tanzania

Yusto J Shine* [1,2], Michael M Msabi[1] and Jagarlamudi Seetharamaiah[1]
[1]*Department of Geology, University of Dodoma, P.O. Box 259, Dodoma, Tanzania*
[2]*Geological Survey of Tanzania, P.O. Box 903, Dodoma, Tanzania*
**Corresponding author e-mail: yustojoseph@gmail.com*
Co-authors' e-mail addresses: mmsabi@yahoo.com, jseetharamaiah@gmail.com
Received 20 Jul 2022, Revised 27 Sep 2022, Accepted 30 Sep 2022, Published Sep 2022
DOI: https://dx.doi.org/10.4314/tjs.v48i3.16

Abstract

This paper presents the mineralogy and chemical composition including iron ore impurities to ascertain its suitability for industrial applications. The Asanje iron ore deposit is hosted in Precambrian volcano-sedimentary rocks in the Mayamaya-Hombolo Belt in Dodoma region, within the Lake Nyanza Superterrane. Iron ores are found in two parallel ridges trending NW-SE. Ridge I occurs as vein and banded hematite-type ore and Ridge II as massive-type ore. A total of 24 ore samples were analysed for major and trace elements by XRF and petrographic studies by optical microscopy and XRD. The XRD results revealed that hematite and goethite are the main components and quartz is the gangue mineral in the iron ores. The XRF data shows the Fe_2O_{3t} content ranges from 20.8 to 87.3 wt% with an average of 52.7 wt%. The average concentrations in wt% of impurities such as SiO_2, Al_2O_3, P_2O_5 and S are 37.9, 0.9, 1.2, and 0.2, respectively. By comparison, Ridge II has greater iron content (30.5–87.3 = Avg. 64.66 wt% Fe_2O_{3t}) than Ridge I (20.8–78.22 = Avg. 48.68 wt% Fe_2O_{3t}). Based on the chemical composition, the quality of iron ore is categorised as low to medium grade, and can be used in metallurgical and cement industries.

Keywords: Mineralogy, Geochemistry, Asanje Iron ore deposit, Mayamaya-Hombolo Belt, Tanzania

Introduction

In recent years, various aspects of iron ore deposits are attracting the attention of different researchers, because of the increasing global demands for iron ore resources (Simonson 2003, 2011, Fru et al. 2018, Duuring et al. 2020). The exploitation of existing iron ore deposits is beneficial to reach the demands of expanding Tanzania's economy (Muwanguzi et al. 2012). Geologically, Tanzania is endowed with vast mineral resource deposits, iron ore deposits being among them (Kabete et al. 2012, Leger et al. 2015, Pitfield 2015). The iron deposits in Tanzania are located within the Archaean Craton, Palaeoproterozoic Usagaran, Ubendian, and Neo-Proterozoic Mozambique Mobile Belt (Kabete et al. 2012, Leger et al. 2015). The most prominent iron ore in Tanzania was reported by Liangzhong (2013), known as Liganga iron ore that occurs within the Ubendian Belt. The Liganga iron ore mainly consists of magnetite with high values of vanadium and titanium as by-products and has an estimated reserve of about 120 million tonnes. The high values of Ti and V concentrations of the Liganga iron ore make this deposit difficult for further exploitation (Liangzhong 2013).

Notably, the Tanzania Archaean Craton is divided into superterranes and sub-terranes, based on both geological and geophysical

knowledge available (Kabete et al. 2012). Among the superterranes, the Lake Nyanza Superterrane (LNST) hosts iron ore deposits extending from the northwest (Geita) to the southeast (Asanje). The LNST that includes the Singida-Mayamaya Terrane is mainly composed of granites, granulites, and migmatite gneisses that are intruded by dolerite/diorite and pegmatite dykes; this terrane hosts several iron ore deposits including the Asanje iron ore deposit located within the Mayamaya-Hombolo belt (Kabete et al. 2012, Pitfield et al. 2015, Thomas et al. 2016). The dating conducted on the LNST rock units, especially on the Singida-Mayamaya Terrane, indicates that it is younger (2681 Ma) than the Dodoma Basement Superterrane (2820 Ma) (Thomas et al. 2016).

The Asanje iron ore deposit is located approximately 45 km north of Dodoma along the southern margin of the Singida-Mayamaya Terrane in the Mayamaya-Hombolo Belt, between the coordinate latitudes 05º44′ 8.02″ S to 05º48′0.98″ S and longitudes 35º41′ 21.50″ E to 35º46′49.0″ E (Figure 1). These iron ore bodies are hosted in Precambrian volcano-sedimentary rocks, which are predominantly composed of ferruginous quartzites, ironstones, micaceous quartzites, quartz, and feldspathic schists (Figure 2, Nkotagu 1996, Leger et al. 2015, Shemsanga et al. 2018). The Asanje iron ore deposit is understudied in terms of grade, impurities, subsurface structural trend, and suitability for industrial uses. The primary aim of this study is to describe the new iron ore in the Dodoma District and present comprehensive interpreted data that are based on the results obtained from petrography, X-Ray Diffractometry (XRD), and X-Ray Fluorescence (XRF) spectrometry analyses to ascertain its suitability as a raw material for industrial applications.

Materials and Methods

The petrographic, XRD, and XRF studies have been carried out for iron ore samples from the Asanje area at the Geological Survey of Tanzania (GST) Laboratory. The XRF spectrometry was used for major and trace elements determination and the complimentary XRD analyses were used for determining mineral phases, petrological microscopy for mineral identification, and high-resolution magnetic image was used for structural interpretation. The high-resolution aeromagnetic data was acquired by GST in 2013 with a terrain clearance of 60 m and line spacing of 250 m.

Sampling, sample preparation, and analyses

A total of 24 representative iron ore samples were collected from the existing active mining pits located along the two ridges (I and II). The samples were randomly collected by cross-cutting the two ridges that are oriented NW-SE direction. About 2 kg of each sample was crushed and sieved to below 75 µm for mineralogical and chemical analysis. All samples were split into four portions for petrographic analysis, gold assay, XRF, and XRD studies at the GST laboratory. A coning and quartering method was performed to get a representative sample for the different methods of study. In addition, the samples for the petrographic study were sawed into smaller portions for polished section preparation. The samples for gold analysis were homogenized into portions of 50 g to be analysed by fire assay with atomic absorption spectrometry finish.

A petrological microscope was used to determine the major and gangue mineral associations. The polished section was placed on the stage of optical light microscope-OPTIKA version 1.1.0, B-600, POL-1, 12 V with 50 W, which is connected to the electric plug. The examination was started at the lower magnification of five and then was increased to 50 times.

The XRD is a fast and reliable method of phase identification and quantification of bulk minerals present in iron ore (see De Andrade et al. 2016). The individual mineral analysis was carried out by XRD; a Bruker AXS Phaser A26-X1-A2B0D2C made in Germany with Cu anode wavelength of 1.540598 Å Cu-Ka1, scan type coupled two theta angle of incidence and X-ray generator of 30 kV with 10.0 mA.

Major, minor, and trace elements were determined by X-Ray Fluorescence (EDXRF) MiniPal 4 Energy Dispersive 12-position sample system with a detection limit of 0.01 wt%. About 10 grams of sample was homogenized and placed into the plastic sample cup and finally placed into the machine to determine the elemental composition of the ore. The results were given in percentage and ppm for major and trace elements, respectively.

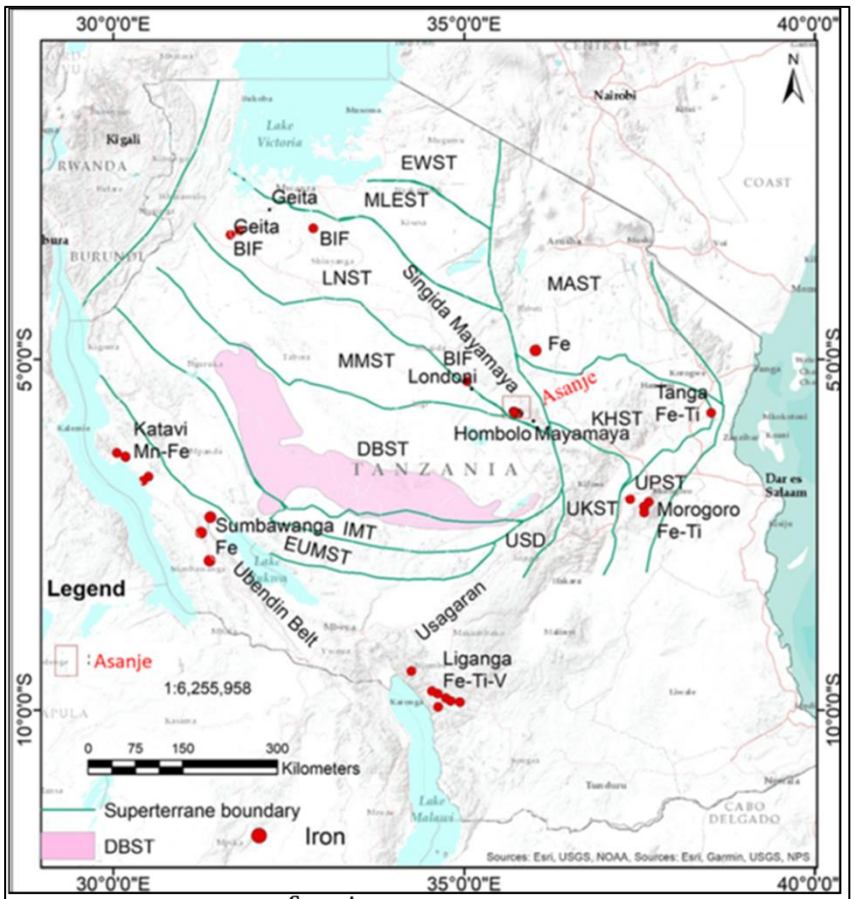

Superterrane

LNST Lake Nyanza Superterrane	**USD** Usagara Domain
MLEST Mwanza Lake Eyasi Superterrane	**UKST** Usagara Ukaguru Superterrane
MMST Moyowosi Manyoni Superterrane	**UPST** Uluguru Pare Superterrane
DBST Dodoma Basement Superterrane	**KHST** Kilindi Handeni Superterrane
IMT Isanga Mtera Terrane	**MAST** Mbulu Masai Superterrane
EUMST East Ubendian Mtera Superterrane	

Figure 1: Locations of iron ores occurrences in Tanzania (adapted from Kabete et al. 2012).

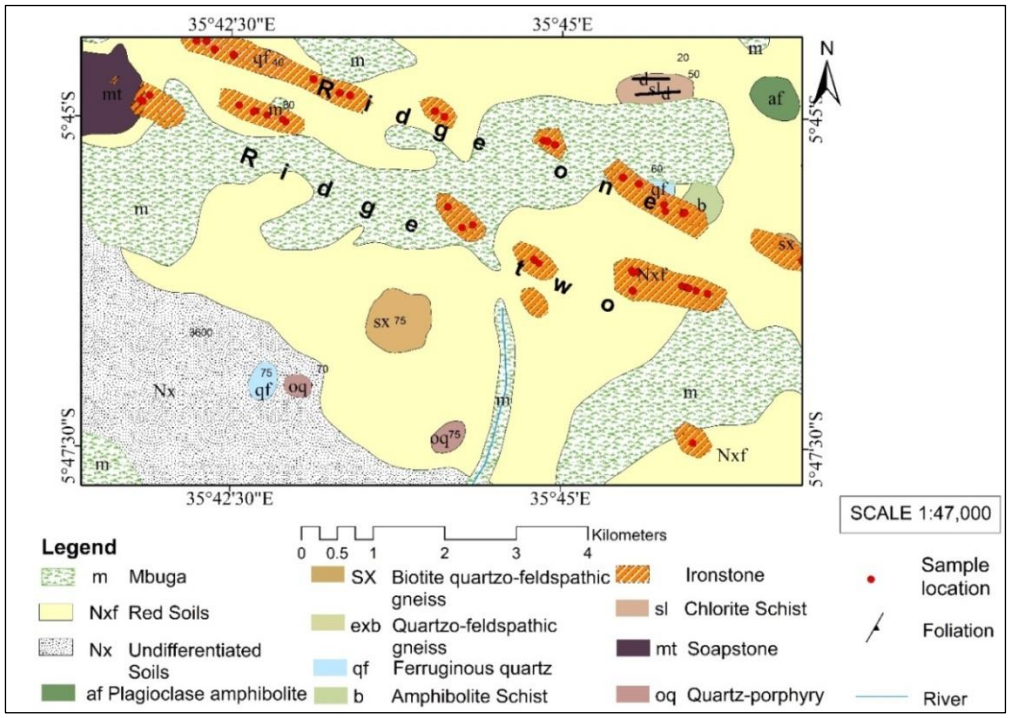

Figure 2: Local geological map of the study area (see inset in Figure 1) with the location of the sample points in Ridge I and Ridge II of the study area.

QA/QC samples were analysed (standard DC73005-56.60 wt% for Fe, blank (marble) and duplicates as per QA/QC standard procedures. The results showed that the accuracy, reproducibility, and sensitivity had acceptable ranges of QA/QC standards (Figure 3).

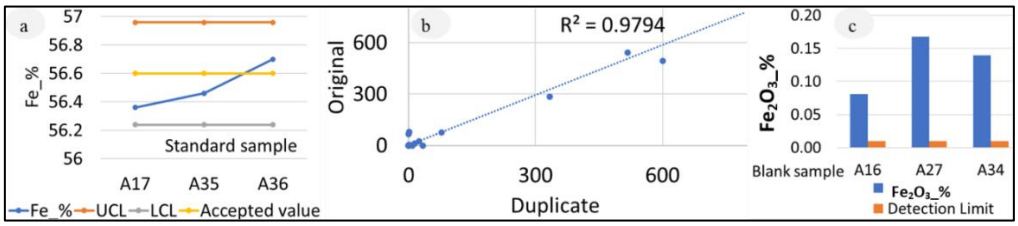

Figure 3: QA/QC plots. (a) Iron ore standard with standard deviation (std) = 0.2, blue (Fe %), yellow, red, and grey lines indicate analysed value, given value, upper control limit (UCL), and lower control limit (LCL), respectively, (b) original and duplicate samples with correlation coefficient (R^2 = 0.9794), and (c) blank sample (blue bar = Fe value and red bar = detection limit).

Results and Discussion

Structural trend of the iron ore body

The total magnetic intensity was used to delineate the structural trend of the iron ore bodies (Figure 4A and B). Figure 4B indicates that Ridge I and Ridge II iron ore bodies are confined along the direction of lineaments and shear zones. The ore body shows a NW-SE trending direction conversely to dolerite dykes, which is striking in a NE-SW direction. According to Kabete et al. (2012), there are linear belts of high

magnetic anomalies trending NW-SE from Moyowosi-Manyoni and also in Dodoma basement Superterrane. The high iron values ranging from 20 to 88 wt% Fe_2O_{3t} are collinear with the higher magnetic bodies (Figure 4).

Occurrence of iron ore

Based on field observations, the iron ore at the Asanje prospect occurs as banded hematite, limonitic banded hematite, goethite vein, and massive/hard hematite (Figure 5A, B, C and D). The thickness of the individual bands differs from a few mm to 6 cm and further varies onto veinlet's/lenses and massive ore (Figure 5). In massive ore, tightly packed fine-grained hematite is intricately associated with other silica (Figure 5D) causing very fine intergranular micropore spaces. They are generally rich in goethite, kaolinite, and quartz.

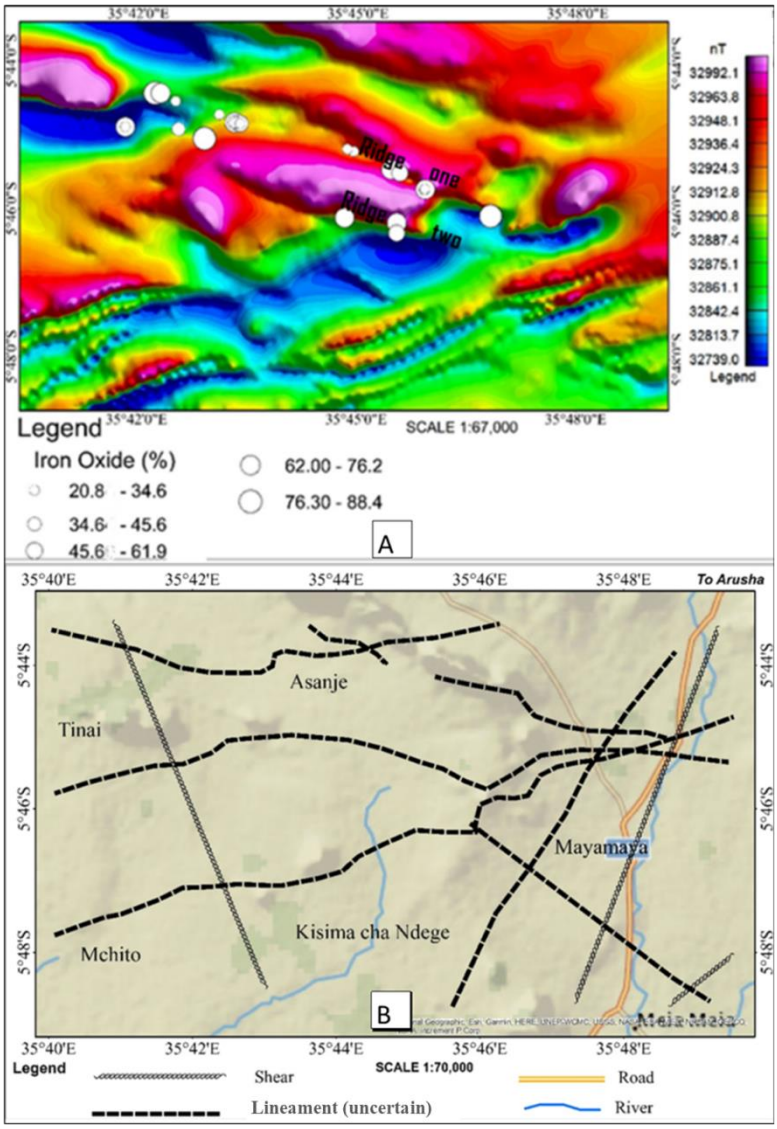

Figure 4: (A) High-resolution magnetic map (contoured nT) showing iron ore values (white circles) and trend of the ore body and (B) interpreted lineaments and shear zones of the study area.

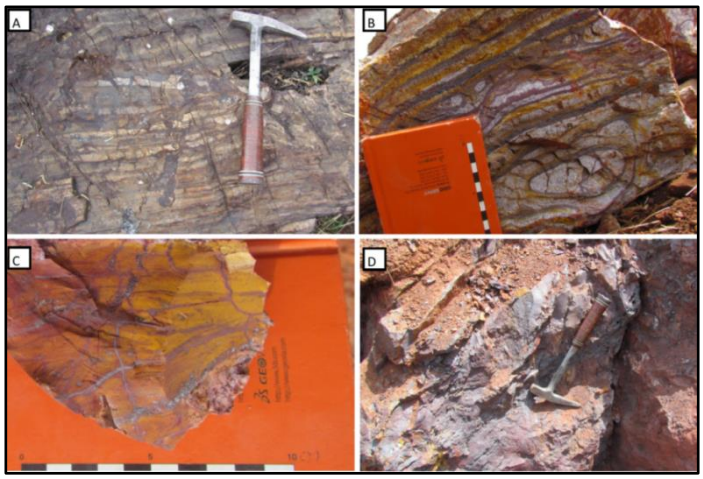

Figure 5: Close-up views (photographs) of iron ore occurrences from quarry faces. (A) banded hematite with the coarse crystal of quartz bands in Ridge I (B) limonitic banded hematite in Ridge I, (C) goethite vein ore in Ridge I, and (D) massive hematite ore in Ridge II.

Petrographic studies

The polished thin sections revealed that hematite and goethite are major ore minerals and bornite, covellite, kaolinite, and quartz as accessory minerals (Figure 6). The Ridge II samples have more hematite and goethite as major ore minerals, whereas Ridge I samples show more hematite, but have less amounts of goethite. A few numbers of crystals of silicate grains occur as inclusions within the ore minerals. The samples have different shapes of grains, which include larger grains of hematite with dark inclusions of quartz and microcrystalline structures. In all samples, variable contents of gangue minerals are noted indicating that the iron deposit formed under different natural conditions similar to the iron ores mineralization of Gandhamardan Hill in India (Bhattacharya and Ghosh 2012).

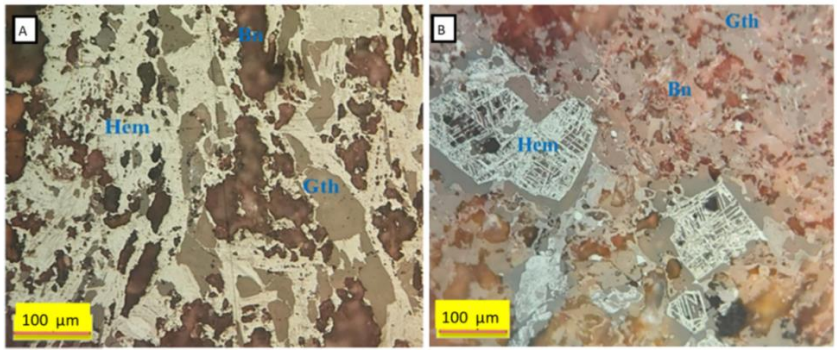

Figure 6: Photomicrograph (under reflected light) of iron ore showing (A) goethite and hematite as main minerals and bornite as gangue mineral in Ridge II and (B) goethite and hematite as the main minerals and bornite in Ridge I (Hem-Hematite, Gth-Goethite, Bn-Bornite).

XRD results

The Asanje iron ore is mainly composed of hematite and goethite with quartz as gangue minerals (Figure 7). These results are similar to the iron ore samples from Quadrilátero Ferrífero in southeastern Brazil (De Andrade et al. 2016). Furthermore, these results corroborated with the iron ore results

from Bellary-Hospet sector in India (Rao et al. 2009). Additionally, the XRD results of the iron ores showed that Ridge I has 18.7% hematite, goethite 10.9%, and 70.4% quartz minerals, whereas Ridge II has 48.5% hematite, goethite 20.3%, and 31.2% quartz (Figure 7). Therefore, the XRD results reaffirmed that the iron ores of Ridges I and II differ in their mineralogical compositions.

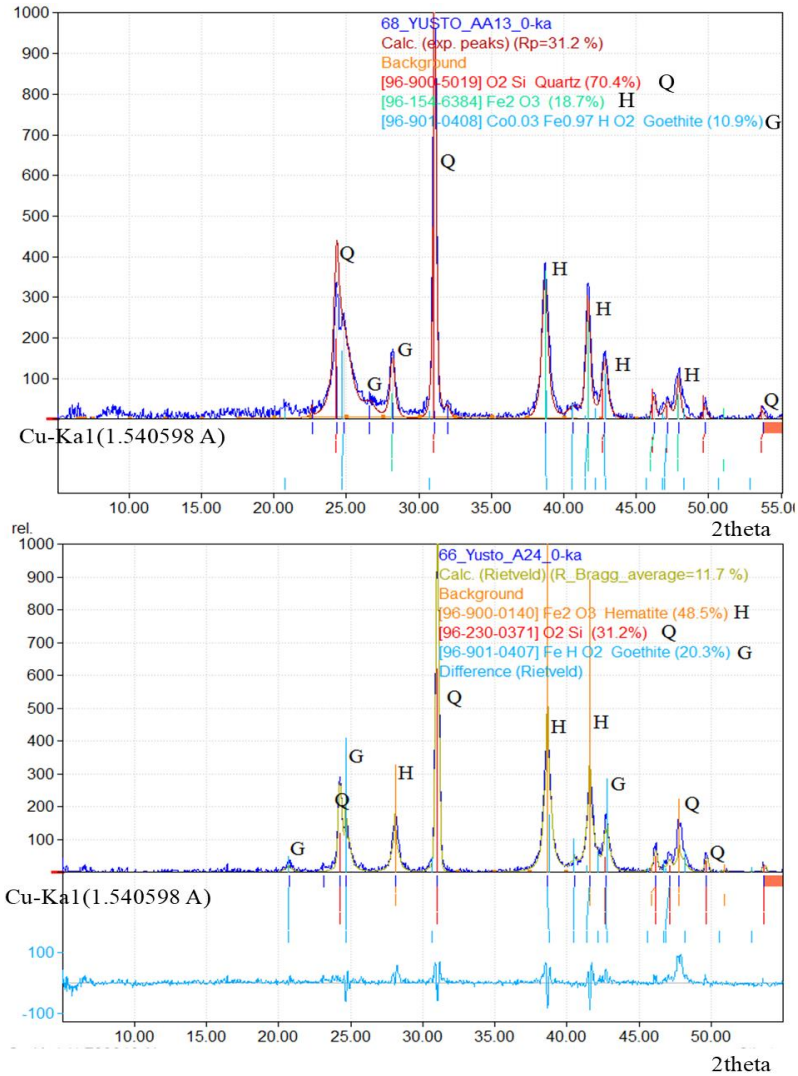

Figure 7: XRD patterns of the iron ore sample numbers (A13) in Ridge I and (A24) in Ridge II (H = Hematite, G = Goethite, and Q = Quartz).

Geochemistry of the iron ore

According to Mukhopadhyay et al. (2008), the quality of iron ores and their variability for economic exploration is mainly controlled by their geochemical characteristics. Diagnostic elemental groups of major and minor elemental associations can be used to distinguish the variations of iron ores (Rao et al. 2009, Pownceby et al. 2019, Grunsky and Caritat 2019). The most important elements and components of consideration in iron ores are the percentages of Fe (total Fe reported as wt% Fe_2O_{3t}), gangue mineral components (SiO_2 and

Al_2O_3), and percentages of P and S (Grunsky and Caritat 2019); these elements with their respective percentages are presented in Table 1. These elements are important because the amount of each element in iron ore affects the quality of the product produced at the end, for example, excess phosphorus increases the cost of steelmaking, and makes steel brittle (see Pownceby et al. 2019).

The iron ores at Asanje in two ridges can be considered as economically viable prospect. Notably, Ridge II has higher values of Fe_2O_{3t} (30.5–87.3 = Avg. 64.7 wt%) compared to that of Ridge I (20.8–78.2 = Avg. 48.7 wt%). Overall, the Asanje iron ore indicates low- to medium-grade iron ore similar to the Muko iron ore in Uganda reported by Muwanguzi et al. (2012). The marked enrichment of iron in all ore samples is accredited to the effective weathering of SiO_2, MgO, and CaO conform to the iron ore of the Singhbhum Craton in India (Mukhopadhyay et al. 2008). The values of impurities of the Asanje iron ore range from 6.1–72.3 wt% SiO_2, 0.2–2.7 wt% Al_2O_3, and 0.1–1.7 wt% P_2O_5.

Using a regression analysis plot (Figure 8) helps to show that SiO_2 in the ore decreases with the increase of $Fe_2O_{3t,}$ therefore having a strong negative correlation with iron ores. By using these results of the regression analysis, the iron ores can be grouped into two categories: the one with low silica as massive hematite medium-grade ore, while the second with high silica as banded hematite or simple low-grade ore.

Table 1: Analytical results of major elements (in wt%) of the iron ore deposit in Ridge I and Ridge II

Ridge I	Sample ID	Fe_2O_{3t}	Fe	SiO_2	Al_2O_3	S	P_2O_5	CaO	K_2O	TiO_2	MgO	Mn
	A01	77.4	54.2	13.9	1.4	0.2	1.4	0.2	0.2	0.6	0.2	0
	A03	74.5	52.1	16.5	0.7	0.1	1.4	0.2	0.1	0.6	0.3	0.1
	A04	42.0	29.4	53.0	0.3	0.2	1.6	0.2	0.1	0.2	0.2	0
	A05	74.7	52.3	13.2	0.7	0.2	1.4	0.2	0.1	0.7	0.3	0
	A06	58.0	40.6	28.8	2.7	0.3	1.5	0.2	0.1	0.2	0.3	0.1
	A07	29.4	20.6	63.5	0.4	0.1	1.4	0.2	0	0.1	0.1	0.1
	A09	44.2	30.9	43.9	0.7	0.1	1.3	0.2	0.1	1.3	1.7	0.1
	A11	30.9	21.6	63.5	0.2	0.1	1.6	0.1	0	0.2	0.1	0
	A12	55.4	38.8	34.9	0.6	0.2	1.5	0.4	0.1	0.1	0.9	1.6
	A13	68.7	48.1	20.5	0.6	0.1	1.6	0.2	0.1	0.9	0.4	0.2
	A14	30.6	21.4	63.2	0.3	0.1	1.5	0.2	0	0.2	0.2	0
	A15	20.8	14.6	72.3	0.6	0.1	1.7	0.1	0.2	0.2	0.2	0
	A21	24.6	17.2	64.6	0.3	0.7	1.1	0.4	0	0	0.7	0.8
	A22	25.8	18.0	67.6	0.4	0.2	1.7	0.3	0	0.1	0.6	0.8
	A23	74.9	52.4	12.3	1.5	0.1	1.4	0.4	0.1	0.1	1.0	1.8
	A26	78.2	54.7	13.5	0.4	0.2	1.4	0.2	0.1	0.3	0.4	0
	A30	32.1	22.5	60.8	1.1	0.3	0.2	0.2	0.1	0.1	0.4	0
	A33	34.1	23.9	59.7	1.1	0.2	0.1	0.1	0.1	0.4	0.3	0
	Average	48.7	34.1	42.5	0.8	0.2	1.3	0.2	0.1	0.4	0.5	0.3

Ridge II	Sample ID	Fe_2O_3	Fe	SiO_2	Al_2O_3	S	P_2O_5	CaO	K_2O	TiO_2	MgO	Mn
	A02	67.3	47.1	22.5	2.1	0.2	1.5	0.2	0.1	0.2	0.1	0
	A10	87.3	61.1	6.1	0.7	0.1	1.4	0.1	0.1	0.1	1.8	0
	A24	74.4	52.0	17.7	0.4	0.1	1.1	0.2	0.1	0.1	0	0
	A25	30.5	21.3	52.7	0.3	0.1	1.6	0.2	0.1	0.1	6.5	0
	A31	60.6	42.4	22.9	1.6	0.5	0.1	0.2	0.1	0.1	0.3	0
	A32	67.9	47.5	21.8	1.4	0.4	0.1	0.3	0.1	0.2	0.5	0
	Average	64.7	45.2	24.0	1.08	0.2	1.0	0.2	0.1	0.1	1.5	0.0

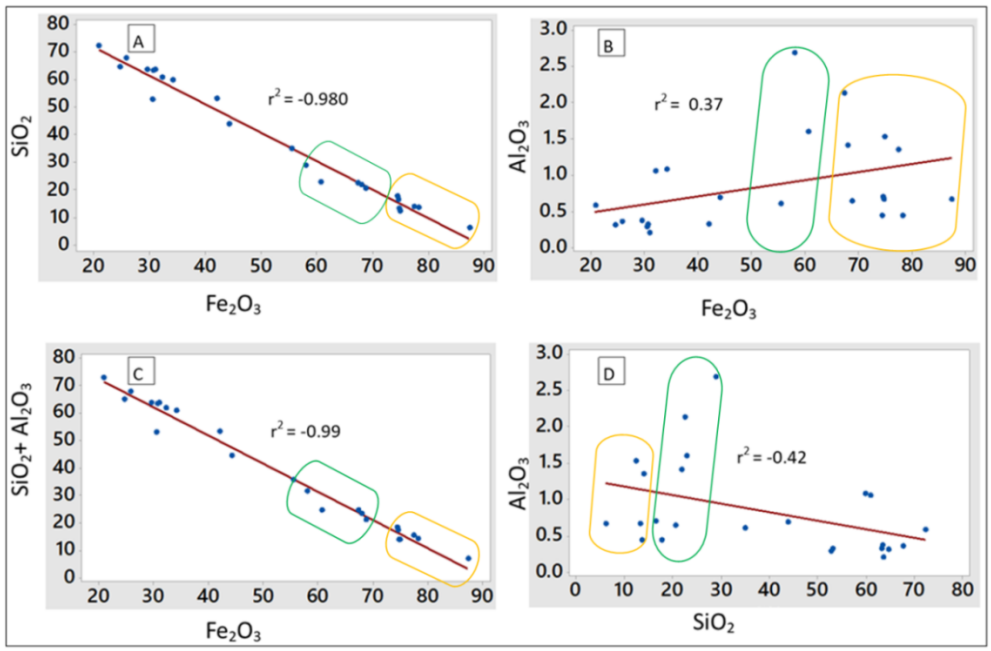

Figure 8: Binary relation of some selected elements (A) SiO_2 versus Fe_2O_{3t} a strong negative correlation, (B) Al_2O_3 versus Fe_2O_{3t} show a weak positive correlation, (C) SiO_2 +Al_2O_3 versus Fe_2O_{3t} a strong negative correlation, and (D) Al_2O_3 versus SiO_2 indicate a negative correlation. The yellow and green rectangles denote medium- and low-grade iron ores, respectively.

The composition of the iron ore within the Mayamaya-Hombolo Belt shows 93 wt% Fe, plus silica, but Al_2O_3 and TiO_2 contents are very low indicating that iron is free of detrital chemical material (terrigeneous). These results are similar to iron ore distributed in Congo Craton (Ganno et al. 2018). The alumina content in the iron ore range from 0.1 to 1.7 wt% Al_2O_3 and shows a very low correlation with either Fe_2O_{3t} or SiO_2 or CaO (Table 2, Figure 8B and C). Al_2O_3 is, however, positively correlated with K_2O, Sr, Cu, and Ba. These results have a similar correlation with iron ore found in Geita-BIF, which indicates little inputs of detrital feldspar or clay to the iron ores (Maboko 2001). Similarly strong negative correlation trend is also observed for a plot of SiO_2 + Al_2O_3 with the iron (Figure 8C). Alumina is mostly less mobile than iron and much less than that of silica and therefore enriched in the residual precipitate. According to Rao et al. (2009), it is suggested that some silica and aluminium coexist in kaolinite, due to a weak correlation between silica and alumina. Other trace elements like arsenic showed a positive correlation (Table 2, r = 0.52) with gold indicating that it is the pathfinder for gold; this co-correlation is similar to the study conducted in Central Dodoma for gold mineralization (Kabete et al. 2012). The amount of phosphorus content in the iron ore from collected samples in the study area ranged from 0.1 to 1.7%; these values are moderately low compared to 1.395% of average phosphorus present in the Agbaja iron ores (Ofoegbu 2019). Also, the phosphorus content is similar to the Quadrilátero Ferrífero iron ore (Brazil) with phosphorus content ranging from 1.13 to 1.70 wt% P_2O_5 (Spier et al. 2019).

Table 2: Pearson Product correlation coefficient values for major and some trace elements

	SiO_2	Fe_2O_{3t}	Al_2O_3	SO_3	P_2O_5	CaO	K_2O	TiO_2	MgO	Cr	V	Mn	As	Au
SiO_2														
Fe_2O_3	-1.00													
Al_2O_3	-0.40	0.37												
SO_3	0.07	-0.10	0.21											
P_2O_5	0.02	0.00	-0.30	-0.60										
CaO	-0.10	0.03	0.16	0.34	-0.10									
K_2O	-0.70	0.65	0.51	-0.10	0.00	0.00								
TiO_2	-0.30	0.27	0.00	-0.20	0.10	-0.20	0.32							
MgO	0.06	-0.10	-0.20	-0.10	0.16	0.08	-0.10	0.00						
Cr	0.00	0.01	0.00	0.07	0.17	0.83	0.00	-0.30	0.03					
V	-0.30	0.20	0.00	-0.20	0.17	0.05	0.16	0.43	0.75	-0.10				
Mn	0.00	0.01	0.00	0.07	0.17	0.83	0.00	-0.30	0.03	1.00	-0.10			
As	-0.10	0.06	-0.10	0.06	-0.10	0.00	0.02	-0.20	0.59	-0.20	0.51	-0.20		
Au	-0.10	0.11	0.15	0.28	-0.50	0.16	0.15	-0.10	0.00	-0.10	0.00	-0.10	0.52	
Sr	-0.10	0.10	0.63	0.07	0.00	0.15	0.16	0.07	-0.10	0.00	0.11	0.00	0.00	0.04
Pb	-0.10	0.01	0.29	0.51	-0.80	0.04	0.05	-0.20	0.19	-0.20	0.13	-0.20	0.48	0.57
Zn	-0.10	0.02	0.11	0.12	0.24	0.79	0.00	-0.20	0.09	0.86	-0.10	0.86	-0.20	-0.10
Cu	-0.30	0.27	0.56	0.46	-0.50	0.17	0.26	-0.20	-0.10	0.01	0.00	0.01	0.06	0.32
Ba	-0.40	0.41	0.54	-0.10	0.00	-0.10	0.46	0.50	-0.10	-0.30	0.21	-0.30	0.02	0.19
Co	-0.50	0.56	0.29	0.00	0.00	-0.10	0.42	0.00	0.11	-0.10	0.09	-0.10	0.31	0.25

The iron ore deposits of the Asanje-Central Tanzania are compared with other iron ore deposits around the world to assess its economic potential. The comparative results show that the iron ore deposit of the Asanje has similar grades and lower impurities like those iron deposits from the: Carajas-Brazil, Muko-Uganda, Mesabi-USA, Nanfen-China, Bakal-Russia, Donimalai in India, and Hammersley in Australia (Muwanguzi et al. 2012, Zhu et al. 2015, Spier et al. 2019).

Conclusions

Iron ore occurs at Asanje in Dodoma, central Tanzania, and is mainly composed of hematite ore (about 52.8 wt% Fe_2O_{3t}), with goethite, bornite, and covellite as accessory minerals. The gangue content is mainly 37.9 wt% SiO_2 and 0.9 wt% Al_2O_3 and contains low levels of S (0.2 wt%) and P_2O_5 (1.2 wt%). By comparison, relatively, Ridge II has greater iron content compared to Ridge I. The key impurities like phosphorus, sulphur, vanadium, and titanium are low falling within the required limits for smelting iron ores. According to Muwanguzi et al (2012), the world market standards and other iron ore producing and exporting nations, the Asanje iron ore deposit is suitable for metallurgical and cement industries as it ranges from low- to medium-grade iron ore.

Acknowledgement

We express our deep and sincere gratitude to the University of Dodoma and the Geological Survey of Tanzania for financial support and permission to publish this research work.

References

Bhattacharya HN and Ghosh KK 2012 Field and petrographic aspects of the iron ore mineralizations of Gandhamardan Hill, Keonjhor, Orissa and their genetic significance. *J. Geol. Soc. India* 79(5): 497–504.

De Andrade FRD, De Andrade GL and Sousa LFA 2016 Iron ore classification by XRD-Rietveld and cluster analysis. *Geologia USP-Serie Cientifica* 16(2): 19–24.

Duuring P, Angerer T, Hagemann SG and Banks DA 2020 Iron deposits hosted by banded iron-formations in the Yilgarn Craton: Products of Sequential Iron enrichment by Magmatic, Marine and Meteoric fluids. *Ore Geol. Rev.* 116: 103251.

Fru EC, Kilias S, Ivarsson M, Rattray JE, Gkika K, McDonald I and Broman C 2018 Sedimentary mechanisms of a modern banded iron formation on Milos Island, Greece. *Solid Earth* 9(3): 573–598.

Ganno S, Tsozué D, Kouankap Nono GD, Tchouatcha MS, Ngnotué T, Gamgne Takam R and Nzenti JP 2018 Geochemical constraints on the origin of banded iron formation-Hosted iron ore from the Archaean Ntem Complex (Congo Craton) in the Meyomessi area, Southern Cameroon. *Resour. Geol.* 68(3): 287–302.

Grunsky EC and Caritat P de 2019 State-of-the-art analysis of geochemical data for mineral exploration. *Geochem.: Explor. Environ., Anal.* 20(2): 217–232.

Kabete JM, Groves DI, McNaughton NJ and Mruma AH 2012 A new tectonic and temporal framework for the Tanzanian shield: implications for gold metallogeny and undiscovered endowment. *Ore Geol. Rev.* 48: 88–124.

Leger C, Barth A, Mruma A, Falk D, Magigitta M, Boniface N and Myumbilwa Y 2015 Explanatory notes for the mineralogenic map of Tanzania. Geological Survey of Tanzania.

Liangzhong C 2013 *Geological report on detailed exploration of the Liganga vanadium-titanomagnetite field Ludewa District, Njombe Region-Tanzania*.

Maboko M 2001 The geochemistry of banded iron formations in the Sukumaland Greenstone Belt of Geita, northern Tanzania: Evidence for mixing of hydrothermal and clastic sources of the chemical elements. *Tanz. J. Sci.* 27(1).

Mukhopadhyay J, Gutzmer J, Beukes NJ and Hayashi KI 2008 Stratabound Magnetite deposits from the eastern outcrop belt of

the Archaean iron ore group, Singhbhum craton, India. *Transactions of the Institutions of Mining and Metallurgy, Section B: Applied Earth Science* 117(4): 175–186.

Muwanguzi AJB, Karasev AV, Byaruhanga JK and Jönsson PG 2012 Characterization of chemical composition and microstructure of natural iron ore from Muko deposits. *ISRN Mater. Sci.* 2012: 1–9.

Nkotagu H 1996 Origins of high nitrate in groundwater in Tanzania. *J. Afr. Earth Sci.* 22(4): 471–478.

Ofoegbu SU 2019 Characterization studies on Agbaja iron ore: a high-phosphorus content ore. *SN Appl. Sci.* 1(3).

Pitfield JEP 2015 *Explanatory notes of Singida-Dodoma-Handeni mineral potential map, Block A, East-Central Tanzania (scale 1:500,000)*. Dodoma, Tanzania.

Pownceby MI, Hapugoda S, Manuel J, Webster NAS and MacRae CM 2019 Characterisation of phosphorus and other impurities in goethite-rich iron ores–Possible P incorporation mechanisms. *Miner. Eng.* 143: 106022.

Rao DS, Kumar TVV, Rao SS, Prabhakar S and Raju GB 2009 Mineralogy and geochemistry of a low-grade iron ore sample from Bellary-Hospet Sector, India and their implications on beneficiation. *J. Miner. Mater. Characteriz. Eng.* 8(02): 115–132.

Shemsanga C, Muzuka ANN, Martz L, Komakech H and Mcharo E 2018 Indigenous knowledge on development and management of shallow dug wells of Dodoma Municipality in Tanzania. *Appl. Water Sci.* 8(2):59.

Simonson BM 2003 Origin and evolution of large Precambrian iron formations. *Special Papers-Geol. Soc. Am.* 231–244.

Simonson BM 2011 Iron ore deposits associated with Precambrian iron formations. *Elements* 7(2): 119–120.

Spier CA, Levett A and Rosière CA 2018 Geochemistry of canga (ferricrete) and evolution of the weathering profile developed on itabirite and iron ore in the Quadrilátero Ferrífero, Minas Gerais, Brazil. *Mineralium Deposita* 54(7): 983-1010.

Thomas RJ, Spencer C, Bushi AM, Baglow N, Boniface N, de Kock G and Millar I 2016. Geochronology of the central Tanzania Craton and its southern and eastern orogenic margins. *Precambrian Res.* 277: 47–67.

Zhu M, Dai Y, Zhang L, Wang C and Liu L 2015 Geochronology and geochemistry of the Nanfen iron deposit in the Anshan-Benxi area, North China Craton: Implications for ~2.55Ga crustal growth and the genesis of high-grade iron ores. *Precambrian Res.* 260: 23–38.